Journal of Statistical Physics, Vol. 75, Nos. 3/4, 1994

A Monte Carlo Study of Size and Angular Properties of a Three-Dimensional Poisson–Delaunay Cell

Susmit Kumar[1] and Stewart K. Kurtz[2,3]

Received March 26, 1993

On the basis of simulation of 1.2×10^6 three-dimensional Poisson–Delaunay cells, the statistical properties of their size and angular parameters have been studied. The moments of the volume, face area, and edge length distributions are found to be equal to those obtained from the exact expressions of Miles and of Moller. The volume, surface area, and face area distributions can be described by the two-parameter gamma distribution. The normal distribution can be used to describe the distributions of the total edge length of a cell and the perimeter of a face. The edge length distribution has also been studied. The distribution of the angle in a face is found to be in accordance with its theoretical distribution.[4]

KEY WORDS: Voronoi tesselation; Delaunay tesselation; Poisson distribution; gamma distribution; normal distribution.

1. INTRODUCTION

For a Poisson point process in a region R^d (where d denotes the dimensionality of the space) with density of nuclei ρ, the simplex with vertices at the $d+1$ points which contains no Poisson point inside it is called a Poisson–Delaunay cell. Delaunay cells are space-filling and convex. Delaunay cells are triangles in two dimensions and tetrahedra in three dimensions.

Delaunay tesselation is the dual of the Voronoi tesselation.[5] In the Voronoi tesselation, n nucleus points are first generated inside the space R^d

[1] Materials Science and Engineering, University of Cincinnati, Cincinnati, Ohio 45221-0012.
[2] Materials Research Laboratory, Pennsylvania State University, University Park, Pennsylvania 16802.
[3] Electrical and Computer Engineering, Pennsylvania State University, University Park, Pennsylvania 16802.

822/75/3-4-25

0022-4715/94/0500-0735$07.00/0

and then the set of points closer to a nucleus P than the other nuclei is assigned to the nucleus P, thus creating a Voronoi polyhedron associated with nucleus P. Each vertex of a Voronoi polyhedron is equidistant from $d+1$ nucleus points. A vertex of a Voronoi polytope is the circumcenter of the circle in two dimensions (of the sphere in three dimensions). The cell formed by joining the $d+1$ nucleus points associated with a vertex of the Voronoi polytope is called the Delaunay cell.

The Voronoi tesselation has been used as a model in a wide variety of areas —agriculture,[6] biology,[7] physics,[8-15] geography,[16] astrophysics,[17-23] crystallography,[24-28] and zoology and ecology.[29-31] An extensive list of the areas in which this tesselation has been used can be found in Stoyan *et al.*[32] and Okabe *et al.*[33]

Medvedev,[34] Medvedev and Naberukhin,[35,36] Medvedev *et al.*,[37,38] Hitwari *et al.*,[39] and Rustad *et al.*[40] have used the Delaunay tesselation constructed by considering the atom sites as the nucleus points to study the structure of liquids, glasses, and amorphous solids. The Delaunay cells give the characteristics of the local disorder in liquids and amorphous solids. They characterize the holes associated with the four nearest atoms. Ostoja-Starzewski[41] and Ostoja-Starzewski and Wang[42,43] have used the Poisson–Delaunay tesselation to model hetereogeneous materials. Treating the edges of the Delaunay cells as linear elastic rods, they calculated the linear mechanical response of the hetereogeneous materials. Christ *et al.*[44-46] used the random lattice generated by Poisson–Delaunay tesselation as a discrete approximation to a continuum field theory and calculated the properties of quantum field theory. They also calculated the mean values of the topological and size parameters of two-, three-, and four-dimensional Poisson–Delaunay tesselation.

Miles[1,2] and Moller[3] theoretically studied the moments of the parameters of the Poisson–Delaunay cells. Using the expression for the moments of the volumes of the Delaunay cells and theory of residues, Rathie[47] derived an exact expression for the volume of the Delaunay cell in one, two, and three dimensions. Okabe *et al.*[33] have tabulated the moments of important parameters of the two-, three-, and four-dimensional Poisson–Delaunay cells.

The properties of Poisson–Voronoi tesselation have been studied by many researchers[48-68] using the computer simulation. But the properties of the Poisson–Delaunay tesselation are less well studied. We have simulated more than 10^6 two-dimensional polygons in order to study the statistical distributions of the parameters of the two-dimensional Poisson–Delaunay tesselation. Details of the simulation will be given elsewhere.[69] The area distribution of the 2D Poisson–Delaunay cells is found to be in accordance with the exact distribution of Rathie.[47] It is also found that

Table I. Properties of the Parameters of 3D Poisson–Delaunay Tesselation

Parameter	Minimum	Maximum	Mean	SD[a]	Skewness	Kurtosis
Volume	7.010×10^{-5}	1.8448	1.4765	0.1234	0.8649	4.7091
Surface area	0.0276	11.0668	2.3886	1.1031	0.4362	0.7870
Area of a face	0.0015	3.4726	0.5971	0.3319	0.5130	0.8931
Edge length	0.0119	3.2245	1.2369	0.4297	0.0314	−0.3327
Total edge length of a cell	1.0099	15.5598	7.4212	1.6292	0.0551	−0.1108
Perimeter of a face	0.2113	8.6692	3.7106	0.9292	0.0429	−0.1374
Radius (volume)	0.0256	0.7607	0.3040	0.0878	0.1184	−0.1521
Radius (surface area)	0.0469	0.9383	0.4242	0.1005	0.0783	−0.1148
Angle in a face	0.3422°	169.63°	59.984°	23.864°	0.2027	−0.2760

[a] Standard deviation.

a two-parameter gamma distribution (see the appendix) can be used to describe the area distribution of the 2D Poisson–Delaunay cells.

In this study, we have simulated more than 1.2×10^6 three-dimensional Poisson–Delaunay cells to study the statistical distributions of their size and angular parameters. The moments of the volume distribution have been found to be equal to those obtained theoretically by Miles.[1] It has been found that a two-parameter gamma distribution can be used to describe the volume, surface area, and face area of the 3D Poisson–Delaunay cells. The distributions of the total edge length of a cell and the perimeter of a face can be described by a normal distribution. The distribution of the angles between adjacent edges in a face of the 3D Poisson–Delaunay cell has been found to be in accordance with the exact expression of Miles.[4]

The volume V, surface area S and face area, perimeter, and edge length data have been normalized by multiplying these data by ρ, $\rho^{1/2}$, and $\rho^{1/3}$, respectively, where ρ is the nucleus density. The values of equivalent radius for volume and surface area were calculated from $(3V/4\pi)^{1/3}$ and $(S/4\pi)^{1/2}$, respectively. (See Table I.)

2. RESULTS AND DISCUSSION

2.1. Volume Distribution

The kth moment of volume V_d of the d-dimensional Poisson–Delaunay cell is given by the expression[1-3]

$$E(V_d^k) = \frac{\Gamma(d^2/2)\Gamma(d+k)\Gamma((d^2+dk+k+1)/2)\Gamma^{d-k+1}((d+1)/2)}{\Gamma(d)\Gamma((d^2+1)/2)\Gamma((d^2+dk)/2)\Gamma^{d+1}((d+k+1)/2)(2^d\pi^{(d-1)/2}\rho)^k} \times \prod_{i=2}^{d+1} \frac{\Gamma((k+i)/2)}{\Gamma(i/2)} \tag{1}$$

where ρ is the nucleus density and $k = 1, 2, 3, \ldots$.

Using Eq. (1) and theory of residues, Rathie[47] derived the probability distribution function for the volume V_d of the one-, two-, and three-dimensional Poisson–Delaunay cell. In one dimension, V has an exponential distribution with parameter ρ; for $\rho = 1$,

$$f(V) = e^{-V}, \qquad V > 0 \tag{2}$$

In two dimensions, the probability distribution function for the area of Delaunay triangle can be written as[47]

$$f(V) = \left(\frac{8}{9}\right) \pi V K_{1/6}^2 \left(\frac{2\pi V}{3\sqrt{3}}\right), \qquad V > 0 \tag{3}$$

where $K_{1/6}(\cdot)$ is the modified Bessel function of order 1/6.

We find[69] that the area distribution of the 2D Poisson–Delaunay triangles can also be described by a two-parameter gamma distribution ($a = 1.3367$ and $b = 0.3741$).

The volume distribution for the 3D Poisson–Delaunay cells is given by the expression[47]

$$f(V) = A_3 \left\{ PV - \sum_{t=0}^{\infty} Q_t V^{2t+3/2} - \sum_{t=0}^{\infty} R_t V^{2t+5/2} - \sum_{t=0}^{\infty} S_t V^{2t+2} \times [-\ln(B_3 V^2) + T_t] \right\} \tag{4}$$

where

$$A_3 = \frac{560\sqrt{2}}{81\pi}$$

$$B_3 = \frac{27\pi^2}{16}$$

$$P = \frac{B_3 \pi \Gamma(1/4)\, \Gamma(3/4)}{\Gamma(5/6)\, \Gamma(7/6)}$$

$$Q_t = \frac{(-1)^t\, \Gamma^2(-t+1/4)\, \Gamma(-t+1/2)\, B_3^{t+5/4}}{(t+1/4)\, \Gamma(-t+7/12)\, \Gamma(-t+11/12)\, t!}$$

Table II. Comparison of Calculated and Theoretical Moments of the Parameters of the 3D Poisson–Delaunay Tesselation

Parameter		Theory[a]	Simulation
Volume	$E(V)$	0.1477	0.1477
	$E(V^2)$	0.0372	0.0370
	$E(V^3)$	0.0135	0.0133
	$E(V^4)$	0.0064	0.0062
	$E(V^5)$	0.0038	0.0036
	$E(V^6)$	0.0027	0.0024
Area of a face	$E(A)$	$(3/4\pi)^{2/3}\,7(5)^3\,\Gamma(2/3)/(3^5\pi) = 0.597$	0.5971
Edge length	$E(L)$	$(3/4\pi)^{1/3}\,5(7)^3\,\Gamma(1/3)/(3^2 4^4) = 1.237$	1.2369

[a] Miles,[1,2] Moller,[3] Okabe *et al.*,[33] and Eq. (1).

$$R_t = \frac{(-1)^t\,\Gamma^2(-t-1/4)\,\Gamma(-t-1/2)\,B_3^{t+7/4}}{(t+3/4)\,\Gamma(-t+1/12)\,\Gamma(-t+5/12)\,t!}$$

$$S_t = \frac{\Gamma(-t-1/4)\,\Gamma(-t+1/4)\,B_3^{t+3/2}}{(t+1/2)\,\Gamma(-t+1/3)\,\Gamma(-t+2/3)(t!)^2}$$

$$\begin{aligned} T_t = {} & 2\psi(t+1) + \psi(-t-1/4) + \psi(-t+1/4) - \psi(-t+1/3) \\ & - \psi(-t+2/3) + (t+1/2)^{-1} \end{aligned}$$

and $\psi(\cdot)$ is the psi function.

The mean number of vertices and the mean volume of the 3D Poisson–Voronoi cell are 27.09 and 1.000, respectively, and as one 3D Poisson–Delaunay cell is associated with four 3D Poisson–Voronoi cells, the mean volume of a 3D Poisson–Delaunay cell is equal to 4/27.09, i.e., 0.1477. The moments of the volume distribution of the 3D Poisson–Delaunay cells calculated on the basis of simulation of more than 1.2×10^6 cells (Table II) have been found to be equal to those obtained from Eq. (1).

We have found that a two-parameter gamma distribution ($a = 1.5135$, $b = 0.0965$, and mean $ab = 0.1460$) can be used to describe the volume distribution of the 3D Poisson–Delaunay cells. These values of the parameters of the gamma distribution give the value of max $|f_{\rm fit} - f_{\rm obs}|$ as 0.005.[4] The 5% Kolmogorov–Smirnov (KS) limit[70] (i.e., $1.63/\sqrt{n}$, where n is the sample size) is 0.0015. Considering the large sample size (i.e., $n = 1.2 \times 10^6$), this difference in max $|f_{\rm fit} - f_{\rm obs}|$ can be neglected. If we insist on the mean

[4] max $|f_{\rm fit} - f_{\rm obs}|$ is the maximum of the absolute difference between the fitted and the observed cumulative distribution functions.

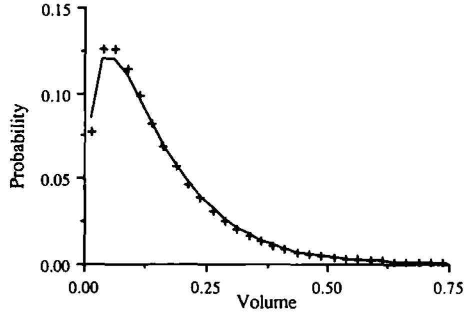

Fig. 1. The probability density distribution of volume of the 3D Poisson–Delaunay cells. Plus signs and solid line denote the simulation data and the best-fit gamma distribution ($a = 1.4749$ and $b = 0.1002$), respectively. The simulation data are based on 1.2×10^6 simulated three-dimensional Poisson–Delaunay cells. The volume data were grouped in equal intervals of width 0.025. See text for the description of the volume normalization factor.

volume being equal to 0.14778, then the best-fit gamma distribution has the parameters $a = 1.4749$ and $b = 0.1002$ (Fig. 1), and max $|f_{\text{fit}} - f_{\text{obs}}|$ for these values of parameters is 0.008.

2.2. Surface Area

We have found that a two-parameter gamma distribution ($a = 4.5530$, $b = 0.5269$, and mean $ab = 2.3990$) can be used to describe the surface area distribution of the 3D Poisson–Delaunay cells. These values of parameters of the gamma distribution give the value of max $|f_{\text{fit}} - f_{\text{obs}}|$ as 0.004. If one

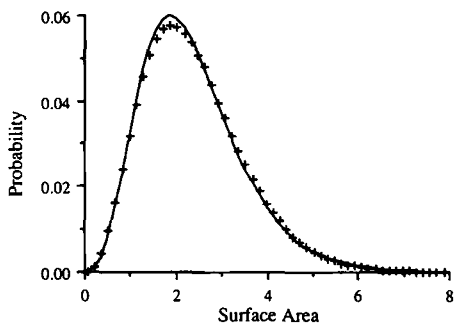

Fig. 2. The probability density distribution of surface area of the 3D Poisson–Delaunay cells. Plus signs and solid line denote the simulation data and the best-fit gamma distribution ($a = 4.7020$ and $b = 0.5080$), respectively. The simulation data are based on 1.2×10^6 simulated three-dimensional Poisson–Delaunay cells. The surface area data were grouped in equal intervals of width 0.15. See text for the description of the surface area normalization factor.

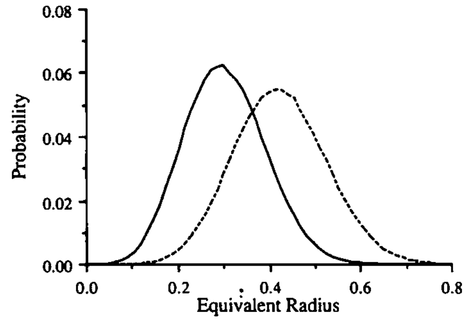

Fig. 3. The probability density distribution of equivalent radius of volume and of surface area for three-dimensional Poisson–Delaunay cells. The values of equivalent radius for volume (solid line) and for surface area (broken line) were calculated from $(3V/4\pi)^{1/3}$ and $(S/4\pi)^{1/2}$, respectively, where V and S denote volume and surface area, respectively. This is based on 1.2×10^6 simulated three-dimensional Poisson–Delaunay cells. The radius data were grouped in equal intervals of width 0.014.

insists on the mean surface area to be equal to the theoretical one, i.e., 2.3886, then the best-fit gamma distribution has the parameters $a = 4.7020$ and $b = 0.5080$ (Fig. 2), and max $|f_{\text{fit}} - f_{\text{obs}}|$ for these values of parameters is 0.007. Figure 3 shows the probability distribution of equivalent radius of volume and of surface area for three-dimensional Poisson–Delaunay cells.

2.3. Face Area

It has been found that a two-parameter gamma distribution with parameters $a = 3.0266$ and $b = 0.1992$ can be used to describe the face

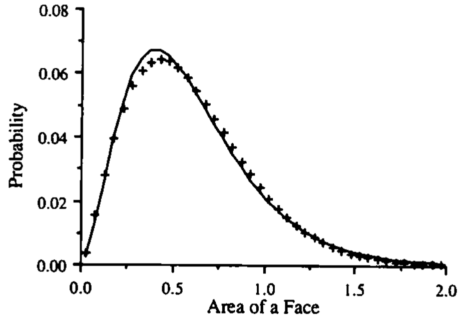

Fig. 4. The probability density distribution of face area of the 3D Poisson–Delaunay cells. Plus signs and solid line denote the simulation data and the best-fit gamma distribution ($a = 3.0266$ and $b = 0.1992$), respectively. The simulation data are based on 1.2×10^6 simulated three-dimensional Poisson–Delaunay cells. The face area data were grouped in equal intervals of width 0.05. See text for the description of the face area normalization factor.

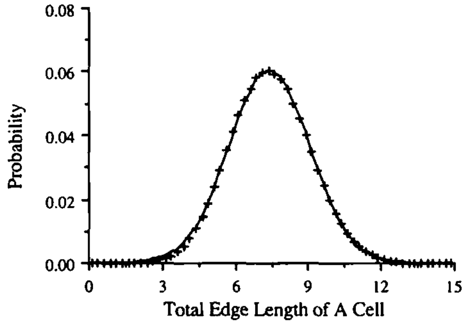

Fig. 5. The probability density distribution of the total edge length of a 3D Poisson–Delaunay cell. Plus signs and solid line denote the simulation data and the best-fit normal distribution ($\sigma = 1.6507$ and $\mu = 7.4212$), respectively. The simulation data are based on 1.2×10^6 simulated three-dimensional Poisson–Delaunay cells. The cell perimeter data were grouped in equal intervals of width 0.25. See text for the description of the perimeter normalization factor.

area distribution of the 3D Poisson–Delaunay cells (Fig. 4). The value of max $|f_{\text{fit}} - f_{\text{obs}}|$ for these parameters of the gamma distribution is 0.009.

2.4. Total Edge Length of a Cell and Perimeter of a Face

It has been found that the normal distribution can be used to describe the distributions of the total edge length of a cell (Fig. 5) and of the perimeter of a face (Fig. 6). The σ and μ parameters of the normal distribu-

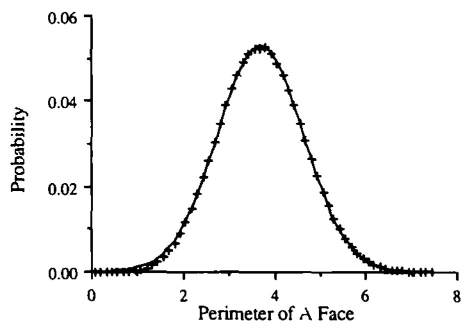

Fig. 6. The probability density distribution of perimeter of a face of the 3D Poisson–Delaunay cell. Plus signs and solid line denote the simulation data and the best-fit normal distribution ($\sigma = 0.9426$ and $\mu = 3.7106$), respectively. The simulation data are based on 1.2×10^6 simulated three-dimensional Poisson–Delaunay cells. The perimeter of the face data were grouped in equal intervals of width 0.125. See text for the description of the perimeter normalization factor.

tions for these two distributions are (1.6507, 7.4212) and (0.9426, 3.7106), respectively. The values of max $|f_{\rm fit} - f_{\rm obs}|$ for these parameters of the gamma distribution are 0.006 and 0.005, respectively.

2.5. Angle in a Face

The dihedral angle is defined as the angle between two faces of a cell, measured in a plane perpendicular to both the faces. For the 3D Poisson–Voronoi cell, the joint density of two (arbitrary) dihedral angles α, β (Fig. 8) at a random edge is[4]

$$f(\alpha, \beta) = \left(\frac{64}{3\pi^2}\right) \sin^2\alpha \sin^2\beta \sin^2(\alpha+\beta) \tag{5}$$

$$(0 \leqslant \alpha \leqslant \pi, \quad 0 \leqslant \beta \leqslant \pi, \quad \alpha + \beta \geqslant \pi)$$

By integrating over β, one gets the dihedral angle distribution as a function of only one dihedral angle,

$$f(\alpha) = \left(\frac{4}{3\pi^2}\right) [2\alpha(2+\cos 2\alpha) - 3 \sin 2\alpha] \sin^2\alpha \tag{6}$$

$$(0 \leqslant \alpha \leqslant \pi)$$

The angle A in a face of the 3D Poisson–Delaunay cell is equal to $(\pi - \alpha)$. Therefore, the distribution of angle A is given by the expression

$$f(A) = \left(\frac{4}{3\pi^2}\right) [2(\pi - A)(2+\cos 2A) + 3 \sin 2A] \sin^2 A \tag{7}$$

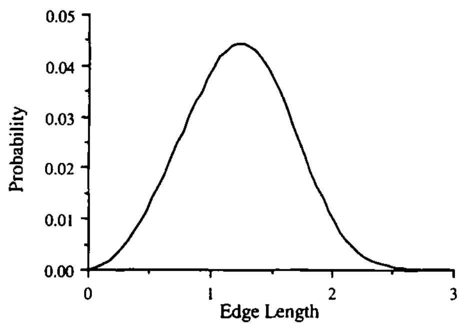

Fig. 7. The probability density distribution of edge length of three-dimensional Poisson–Delaunay cells. This is based on 1.2×10^6 simulated three-dimensional Poisson–Delaunay cells. The edge length data were grouped in equal intervals of width 0.05. See text for the description of the edge length normalization factor.

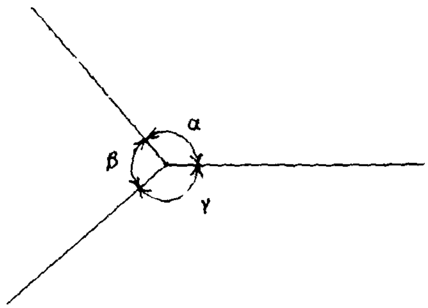

Fig. 8. Dihedral angles at a random edge of a 3D Poisson–Voronoi cell. $\alpha+\beta+\gamma=2\pi$.

The mode of the function $f(A)$ is the solution of the equation

$$2\sin A - 2\sin 3A - \sin 2A\cos A - 4(\pi - A)\cos A - 2(\pi - A)\cos 3A = 0$$

i.e., $A = 55.637°$.

The expected value and the standard deviation of the dihedral angle are

$$\langle A\rangle = \frac{\pi}{3} = 60°$$

$$\text{Variance }(A) = \frac{\pi^2}{18} - \frac{3}{8}$$

$$\text{Standard deviation }(A) = 23.853°$$

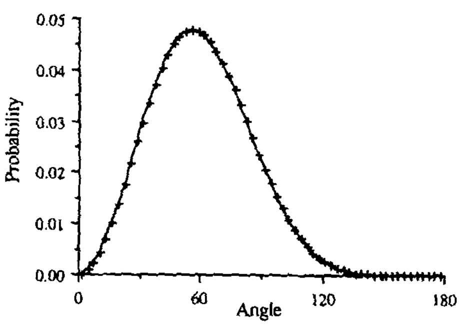

Fig. 9. Distribution of the angle in the face of the 3D Poisson–Delaunay cell. Plus signs and solid line denote the simulation data and the theoretical expression of Miles[4] [Eq. (7)], respectively. The simulation data are based on 1.2×10^6 simulated three-dimensional Poisson–Delaunay cells. The angle data were grouped in equal intervals of width 3°.

As shown in Table I and Fig. 9, the distribution of the angle in a face of a 3D Poisson–Delaunay cell, calculated on the basis of 1.2×10^6 cells is in accordance with the Eq. (7).

3. CONCLUSION

More than 1.2×10^6 three-dimensional Poisson–Delaunay cells were simulated to study the statistical properties of size and angular parameters of the Delaunay cells. The moments of the size distributions were found to be equal to those obtained theoretically by Miles,[1,2] and Moller[3] and tabulated in Okabe *et al.*[33] The volume, surface area, and face area distributions can be approximately described by a two-parameter gamma distribution. A normal distribution can be used to describe the distributions of the total edge length of a cell and the perimeter of a face of the cell. The edge length distribution was also studied. The distribution of the angle in a face was found to be in accordance with the exact expression of Miles.[4]

APPENDIX

(i) The gamma distribution with two parameters a and b is described by

$$P_{x,x+dx} = \frac{x^{a-1}}{b^a \Gamma(a)} e^{-x/b}\, dx, \qquad x > 0$$

where mean and variance are ab and ab^2, respectively.

(ii) The normal distribution with two parameters σ (standard deviation) and μ (mean) is described by

$$P_{x,x+dx} = \frac{1}{\sigma(2\pi)^{1/2}} \exp\left[- \frac{(x-\mu)^2}{2\sigma^2} \right] dx$$

ACKNOWLEDGMENTS

Financial support for this work was provided by Murata Corporation. Computations were performed on the IBM 3090 at the Center for Academic Computing, Pennsylvania State University, whose assistance is gratefully acknowledged.

REFERENCES

1. R. E. Miles, The random division of space, Adv. Appl. Prob. *Suppl.* **1972**:243–266.
2. R. E. Miles, A synopsis of 'Poisson flats in Euclidean spaces,' in *Stochastic Geometry*, E. F. Harding and D. G. Kendall, eds. (Wiley, New York, 1974).
3. J. Moller, Random tessellations in R^d, *Adv. Appl. Prob.* **21**:37–73 (1989).
4. R. E. Miles, Australian National University, Australia, Private communication (1992).
5. G. Voronoi, *J. Reine Angew. Math.* **134**:198–287 (1908).
6. R. A. Fischer and R. E. Miles, The role of spatial competition between crop plants and weeds. A theoretical analysis, *Math. Biosci.* **18**:335–350 (1973).
7. H. Honda, Geometrical models for cells in tissues, *Int. Rev. Cytol.* **81**:191–248 (1983).
8. A. Rahman, Liquid structure and self-diffusion, *J. Chem. Phys.* **45**:2585–2592 (1966).
9. F. M. Richards, Area, volumes, packing, and protein structure, *Annu. Rev. Biophys. Bioeng.* **6**:151–76 (1977).
10. J. L. Finney, Volume occupation, environment and accessibility in proteins: The problem of the protein surface, *J. Mol. Biol.* **96**:721–732 (1975).
11. P. H. Winterfeld, Ph. d. Thesis, University of Minnesota (1981).
12. E. W. Kaler and S. Prager, A model of dynamic scattering by microemulsion, *J. Colloid Interface Sci.* **86**:359–369 (1982).
13. S. Kumar, Ph. d. Thesis, Pennsylvania State University (1992).
14. M. Kobayashi, H. Maekawa, and Y. Kondous, Calculation of the mean thermal conductivity of a heterogeneous solid mixture with the Voronoi-polyhedron element method, *Heat Transfer: Jpn. Res.* **21**:219–236 (1992).
15. S. Kumar and S. K. Kurtz, Simulation of material microstructure using a 3D Voronoi tesselation: Calculation of effective thermal expansion coefficient of polycrystalline materials, to be published.
16. P. Pathak, Ph. d. Thesis, University of Minnesota (1981).
17. T. Kiang, Random fragmentation in two and three dimensions, *Z. Astrophys.* **64**:433–439 (1966).
18. V. Icke and R. Vande Weygaert, Fragmenting the universe I: Statistics of two-dimensional Voronoi foam, *Astron. Astrophys.* **184**:16–32 (1987).
19. R. Vande Weygaert and V. Icke, Fragmenting the universe II: Voronoi vertices as Abell clusters, *Astron. Astrophys.* **213**:1–9 (1989).
20. S. Yoshioka and S. Ikeuchi, The large scale structures of the universe and the division of space, *Astrophys. J.* **341**:16–25 (1989).
21. V. J. Martinez, B. J. T. Jones, R. D. Tenreiro, and R. Weygaert, Clustering paradigms and multifractal measures, *Astrophys. J.* **357**:50–61 (1990).
22. M. Pierre, Probes for the large scale structures, *Astron. Astrophys.* **229**:7–16 (1990).
23. L. Zaninetti, The Voronoi tessellation generated from different distributions of seeds, *Phys. Lett. A* **165**:143–147 (1992).
24. J. L. Meijering, Interface area, edge length, and number of vertices in crystal aggregates with random nucleation, *Philips Res. Rep.* **8**:270–290 (1953).
25. E. N. Gilbert, Random subdivisions of space into crystals, *Ann. Math. Sttat.* **33**:958–972 (1962).
26. A. L. Mackay, Stereological characteristics of atomic arrangements in crystals, *J. Microsc.* **95**(2):217–227 (1972).
27. P. J. Wray, O. Richmond, and H. L. Morrison, Use of Dirichlet tessellation for characterizing and modelling nonregular dispersions of second phase particles, *Metallography* **16**:39–58 (1983).
28. H. J. Frost and C. V. Thompson, The Effect of nucleation condition on the topology and geometry of two-dimensional grain structures, *Acta Met.* **35**:529–540 (1987).

29. M. Hasegawa and M. Tanemura, On the pattern of space division by territories, *Ann. Inst. Stat. Math.* **28** (Part B):509–519 (1976).
30. M. Hasegawa and M. Tanemura, in *Recent Developments in Statistical Inference and Data Analysis*, K. Matusita, ed. (North-Holland, Amsterdam, 1980), pp. 73–78.
31. M. Tanemura and M. Hasegawa, Geometrical models of territory I. Models of synchronous and asynchronous settlement of territories, *J. Theor. Biol.* **82**:477–496 (1980).
32. D. Stoyan, W. S. Kendall, and J. Mecke, *Stochastic Geometry and Its Application* (Wiley, New York, 1987).
33. A. Okabe, B. Boots, and K. Sugihara, *Spatial Tessellations: Concepts and Applications of Voronoi Diagrams* (Wiley, New York, 1992).
34. N. N. Medvedev, Aggregation of tetrahedral and quartoctahedral Delaunay simplices in liquid and amorphous rubidium, *J. Phys. Condensed Matter* **2**:9145–9154 (1990).
35. N. N. Medvedev and Y. I. Naberukhin, Study of the structure of simple liquids and amorphous soilds by statistical geometry methods, *J. Struct. Chem.* **28**(3):433–446 (1987).
36. N. N. Medvedev and Y. I. Naberukhin, Shape of the Delaunay simplices in dense random packings of hard and soft spheres, *J. Non-Cryst. Solids* **94**:402–406 (1987).
37. N. N. Medvedev, V. P. Voloshin, and Y. I. Naberukhin, Structures of simple liquids as a percolation problem on the Voronoi network, *J. Phys. A: Math. Gen.* **21**:L247–L252 (1988).
38. N. N. Medvedev, V. P. Voloshin, and Y. I. Naberukhin, Structures of simple liquids as a problem of percolation in the Voronoi grid, *J. Struct. Chem.* **30**:253–260 (1989).
39. Y. Hitwari, T. Saito, and A. Ueda, Structural characterization of soft-core and hard-core glasses by Delaunay tesselation, *J. Chem. Phys.* **81**:6044–6050 (1984).
40. J. R. Rustad, D. A. Yuen, and F. J. Spera, The statistical geometry of amorphous silica at lower mantle pressures: Implications for melting slopes of silicates and anharmonicity, *J. Geophys. Res.* **96**:19665–19673 (1991).
41. M. Ostoja-Starzewski, Bounds on constitutive response for a class of random material microstructures, *Computers Structures* **37**:163–167 (1990).
42. M. Ostoja-Starzewski and C. Wang, Linear elasticity of planar Delaunay networks: Random field characterization of effective moduli, *Acta Mech.* **80**:61–80 (1989).
43. M. Ostoja-Starzewski and C. Wang, Linear elasticity of planar Delaunay networks. Part II: Voigt and Reuss bounds, and modification for centroids, *Acta Mech.* **84**:47–61 (1990).
44. N. H. Christ, R. Friedberg, and T. D. Lee, Random lattice field theory: General formulation, *Nucl. Phys. B* **202**:89–125 (1982).
45. N. H. Christ, R. Friedberg, and T. D. Lee, Gauge theory on a random lattice, *Nucl. Phys. B* **210**:310–336 (1982).
46. N. H. Christ, R. Friedberg, and T. D. Lee, Weights of links and plaquettes in a random lattice, *Nucl. Phys. B* **210**:337–346 (1982).
47. P. N. Rathie, On the volume distribution of the typical Poisson–Delaunay cell, *J. Appl. Prob.* **29**:740–744 (1992).
48. H. G. Hanson, Voronoi cell properties from simulated and real random spheres and points, *J. Stat. Phys.* **30**:591–605 (1983).
49. B. N. Boots and D. J. Murdoch, The spatial arrangement of random Voronoi polygons, *Computers Geosci.* **9**:351–365 (1983).
50. J. M. Drouffe and C. Itzykson, Random geometry and the statistics of two-dimensional cells, *Nucl. Phys. B* **235**:45–53 (1984).
51. M. P. Quine and D. F. Watson, Radial generation of *n*-dimensional Poisson processes, *J. Appl. Prob.* **21**:548–557 (1984).
52. D. Weaire and J. P. Kermode, Computer simulation of a two-dimensional soap froth II. Analysis of results, *Phil. Mag. B* **50**:379–395 (1984).

53. D. Weaire, J. P. Kermode, and J. Wejchert, On the distribution of cell areas in a Voronoi network, *Phil. Mag. B* **53**:L101–105 (1986).
54. B. N. Boots, The arrangement of cells in "random" networks, *Metallography* **15**:53–62 (1982).
55. B. N. Boots, Edge length properties of random Voronoi polygons, *Metallography* **20**:231–236 (1987).
56. P. N. Andrade and M. A. Fortes, Distribution of cell volumes in a Voronoi partition, *Phil. Mag. B* **58**:671–674 (1988).
57. H. Hermann, H. Wendrock, and D. Stoyan, Cell-area distributions of planar Voronoi mosaics, *Metallography* **23**:189–200 (1989).
58. G. L. Le Caer and J. S. Ho, The Voronoi tessellation generated from eigenvalues of complex random matrices, *J. Phys. A: Math. Gen.* **23**:3279–3295 (1990).
59. U. Lorz, Cell-area distributions of planar sections of spatial Voronoi mosaics, *Materials Characterization* **25**:297–309 (1990).
60. U. Lorz, Distributions of cell characteristics of the spatial Poisson–Voronoi tessellation and plane sections, in *Geometerical Problems of Image Processings*, Vol. 4, U. Eckhardt, A. Hubler, W. Nagel, and G. Werner, eds. (Akademic Verlag, 1991), pp. 171–178.
61. A. Thorvaldsen, Simulation of 3-D Voronoi polygons, *Materials Sci. Forum* **94–96**:307 (1992).
62. S. Kumar and S. K. Kurtz, Properties of a two-dimensional Poisson–Voronoi tesselation: A Monte Carlo study, *Materials Characterization* **31**:55–68 (1993).
63. S. Kumar, S. K. Kurtz, and D. Weaire, Average number of sides for the neighbors in a Poisson–Voronoi tesselation, *Phil. Mag. B* **69**:431–435 (1994).
64. I. K. Crain, The Monte-Carlo generation of random polygons, *Computers Geosci.* **4**:131–141 (1978).
65. A. L. Hinde and R. E. Miles, Monte-Carlo estimates of the distributions of the random polygons of the Voronoi tesselation with respect to a Poisson process, *J. Stat. Computation Simulation* **10**:205–223 (1980).
66. K. W. Mahin, K. Hanson, and J. W. Morris, Jr., Comparative analysis of the cellular and Johnson–Mehl microstructures through computer simulation, *Acta Met.* **28**:443–453 (1980).
67. S. Kumar, S. K. Kurtz, J. R. Banavar, and M. G. Sharma, Properties of a three-dimensional Poisson–Voronoi tesselation: A Monte-Carlo study, *J. Stat. Phys.* **67**:523–551 (1992).
68. V. Horalek, ASTM grain-size model and related random tessellation models, *Materials Characterization* **25**:263–284 (1990).
69. S. Kumar and S. K. Kurtz, Computer simulation of a two-dimensional Poisson–Delaunay tesselation, to be published.
70. J. D. Gibbons and S. Chakraborti, *Nonparametric Statistical Inference*, 3rd ed., (Marcel Dekker, New York, 1992).